IEEE Access
Multidisciplinary | Rapid Review | Open Access Journal

Received September 14, 2017, accepted October 21, 2017, date of publication October 30, 2017, date of current version February 14, 2018.

Digital Object Identifier 10.1109/ACCESS.2017.2767698

Fault Detection Based on Modified Kernel Semi-Supervised Locally Linear Embedding

YINGWEI ZHANG, (Senior Member, IEEE), YUANJIAN FU, ZHENBANG WANG, AND LIN FENG

The authors are with the State Laboratory of Synthesis Automation of Process Industry, Northeastern University, Shenyang 110819, China

Corresponding author: Yingwei Zhang (zhangyingwei@mail.neu.edu.cn)

This work was supported in part by China's National 973 program under Grant 2009CB320600 and in part by the National Natural Science Foundation of China under Grant 61325015 and Grant 61273163.

ABSTRACT In this paper, a novel approach to fault detection for nonlinear processes is proposed. It is based on a manifold learning called modified kernel semi-supervised local linear embedding. Local linear embedding (LLE) is widely applied to fault detection of complex industrial process. However, the LLE only preserves the local structure information of the sample, which ignores the global characteristics of the original data. The main contributions of the presented approach are as follows: 1) in order to utilize labeled data, the semi-supervised learning is introduced into LLE; 2) the regularization term is added to the calculation of local reconstruction weights matrix to strengthen the anti-noise ability in nonlinear processing; and 3) in order to extract the global and local characteristic of the observation data, the kernel principal component analysis objective function is integrated with the objective function of LLE. Experimental results on the production process of fused magnesia verify the performance of the proposed method.

INDEX TERMS Fault detection, LLE, KPCA, semi-supervised learning.

I. INTRODUCTION

Complex industrial processes are typically subject to disturbances of manual or machine operation. Therefore, it is critical to maintain excellent sensitivity to faults in industrial processes. Currently, the fault detection of cyber-physical system (CPS) has received extensive attention. The cyber-physical system is a multi-dimensional complex system of integrated computing, network and physical world [1]. Such systems commonly exist in both industrial processes and people's daily lives. Fault diagnosis technology is an important method to improve the system reliability and reduce accident risk. A variety of methods for traditional fault diagnosis have been proposed. These traditional methods are, Principal Component analysis (PCA) [2], Independent Component Analysis (ICA) [3], Partial Least Squares (PLS) [4], [5], and Fisher's Discriminate Analysis (FDA) [6], etc.

Recently, manifold learning is applied the field of fault diagnosis, which has been a hot research topic. Roweis and Saul [7] proposed that the local linear embedding manifold learning algorithm is widely utilized. It is mainly employed in a variety of fields, such as data mining, image processing, fault diagnosis and pattern recognition [8]. To tackle the problems of LLE for data mining, image processing and fault diagnosis, some initiatory efforts have been recently taken to develop various improved versions of LLE by means of modifying the formula in LLE. Donoho [9] proposed a local linear embedding algorithm based on Hessian matrix, the local neighborhood in Euclidean space as a Riemannian manifold, embedding feature vector convert eigenvalue problem of Hessian matrix. Xiao Jian proposed a self-organizing local linear embedding algorithm for noise manifold learning and pattern recognition. The expanded LLE has become the most promising technology [10]. In the expanded algorithm of LLE [11], [14], Tsagaroulis [13] proposed kernel locally linear embedding algorithm for quality control. The proposed control chart is available in the detection of outliers, and its control limits are obtained from the analysis of the kernel matrix in the Hilbert feature space. By describing the concept of supervision [12], the labeled training data can be used to guide the traditional LLE to search the k neighboring points around each sample point in the SLLE [17]. Li proposed a feature extraction method based on Gabor wavelet and supervised local linear embedding. Liang proposed a fault recognition method based on supervised incremental locally linear embedding [18]. However, the cost is great for all labeled training data, and it is not easy to implement in industrial processes. Semi-supervised learning can increase the accuracy of the detection and the rationality of the projection points of the low dimensional mapping by using some labeled data and a large number of

inexpensive unlabeled samples. Therefore, the combination of semi-supervised learning and LLE has become the focus of research [19]–[23].

To overcome the insufficient of LLE, in this paper a novel modified kernel semi-supervised LLE method is proposed and applied for fault detection in industrial process. Great efforts were made to improve the algorithm. On one hand, the distance matrix is adjusted by the semi-supervised learning method, making the weight matrix more accurate. On the other hand, in order to strengthen the anti-noise ability in nonlinear data processing, the regularization term is added to the calculation of local reconstruction weights matrix. Ultimately, the kernel LLE (KLLE) algorithm only preserves the local structure information of the sample, but it ignores the global characteristics of the original data [15], [16]. Therefore, the KPCA is adopted into the processing of projection matrix objective function. Taking advantage of KPCA to extract global features, the global and local information of sample data can be extracted completely [24], [25].

The remainder of this article is organized as follows. The LLE method is shown in Section 2. The proposed MK-SSLLE method is presented in Section 3. The process monitoring framework based on MK-SSLLE is developed to realize fault detection in Section 4. The experimental results are shown in Section 5. The conclusion is drawn in Section 6.

II. REVIEWS OF LLE

Given input dataset $\mathbf{X} = [\mathbf{x}_i, \ldots, \mathbf{x}_n]$ and the output dataset $\mathbf{Y} = [y_1, \ldots, \mathbf{y}_n]$.

(1) Find the k nearest neighbors for each sample point $\mathbf{x}_i$ based on the Euclidean distance.

(2) Compute the reconstruction weights matrix $\mathbf{W}_{ij}$ by the k nearest neighbors for each sample point $\mathbf{x}_i$.

According to the following minimum reconstruction error to acquire weights matrix $\mathbf{W}_{ij}$.

$$\min \varepsilon_i(\mathbf{W}) = \sum_{i=1}^{n} \left\| \mathbf{x}_i - \sum_{j=1}^{n} \mathbf{W}_{ij}\mathbf{x}_j \right\|^2$$
$$s.t. \begin{cases} \sum_{j=1}^{n} W_{ij} = 1 \\ \mathbf{W}_{ij} = 0, \quad \mathbf{x}_j \notin N(\mathbf{x}_j),\ j = 1, \ldots, k \end{cases} \tag{1}$$

(3) Compute the low-dimensional embedding.

The low-dimensional embedding y_i may be derived by minimizing the following cost error.

$$\min \varepsilon(\mathbf{Y}) = \sum_{i=1}^{n} \left\| \mathbf{y}_i - \sum_{j=1}^{n} \mathbf{W}_{ij}\mathbf{y}_j \right\|^2$$
$$s.t.\ \mathbf{Y}^T\mathbf{Y} = \mathbf{I}_n \tag{2}$$

The structure of nonlinear manifolds is learned by LLE. In Fig. 1, such as, the input to LLE consists of $N = 2000$ data points sampled from the S-curve manifold. The dimensionality reduction consequence by LLE in Fig. 1(c).

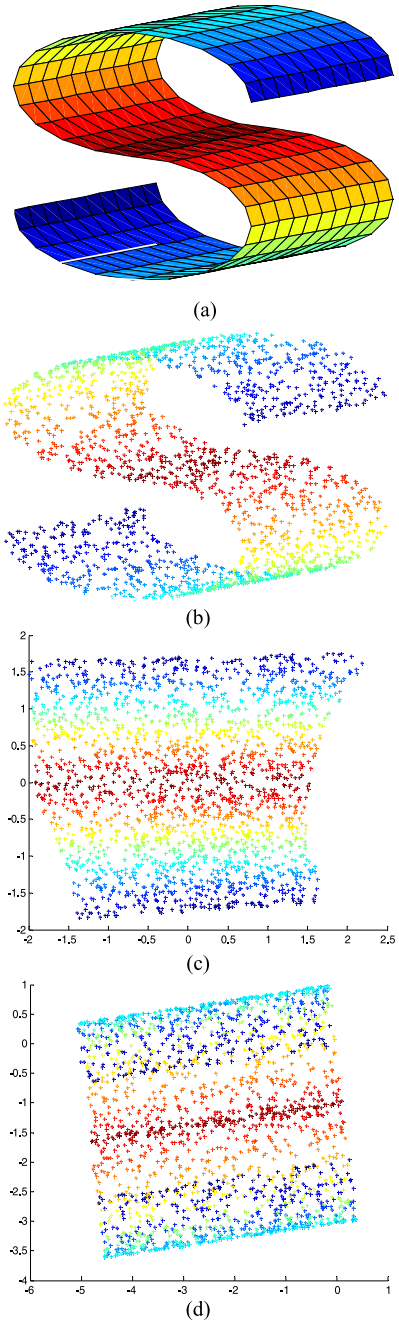

FIGURE 1. (a) S-curve manifold in three-dimensional space, (b) 2000 data points sampled from the S-curve manifold, and (c) dimensionality reduction consequence by LLE from three-dimensional space to two-dimensional space, and (d) dimensionality reduction consequence by PCA.

The dimensionality reduction consequence by PCA in Fig. 1(d). LLE is able to preserve the structure of nonlinear manifolds from Fig. 1(c). For maintaining the structure of local manifold, the reduced dimension result of PCA is not effective from Fig. 1(d).

In this paper, the advantages of these two methods are effectively integrated, so the performance of fault detection is improved.

$$\begin{aligned}\sqrt{\mathbf{S}(i)}\sqrt{\mathbf{S}(j)} &= \sqrt{\frac{1}{k}\sum_{p=1}^{k}\left\|\mathbf{\Phi}\left(\mathbf{x}_i\right)-\mathbf{\Phi}\left(\mathbf{x}_p^i\right)\right\|^2}\sqrt{\frac{1}{k}\sum_{q=1}^{k}\left\|\mathbf{\Phi}\left(\mathbf{x}_j\right)-\mathbf{\Phi}\left(\mathbf{x}_q^i\right)\right\|^2} \\ &= \sqrt{\frac{1}{k^2}\sum_{p=1}^{k}\left(\mathbf{K}_{ii}-\mathbf{K}_{ip^i}-\mathbf{K}_{p^ii}+\mathbf{K}_{p^ip^i}\right)\sum_{q=1}^{k}\left(\mathbf{K}_{jj}-\mathbf{K}_{jq^j}-\mathbf{K}_{q^ij}+\mathbf{K}_{q^iq^i}\right)} \\ &\Rightarrow = \sqrt{\Delta}\end{aligned}$$

III. MODIFIED KERNEL SEMI-SUPERVISED LOCALLY LINEAR EMBEDDING

In an industrial big data pool, there are a variety of modal normal data and a large number of unlabeled normal data. By studying the characteristics of multi-mode data and unlabeled data, the detection accuracy has been improved.

Assume that the standardized process data is $\mathbf{X} = (\mathbf{X}_L, \mathbf{X}_U) \in \mathbf{R}^{m\times n}$, where the dataset $\mathbf{X}_L = [\mathbf{x}_1, \mathbf{x}_2, \ldots, \mathbf{x}_l]$ as labeled data, the number of class labels is c, the number of samples for each class is N_i, $i = (1, 2, \cdots, c)$. The dataset $\mathbf{X}_U = [\mathbf{x}_{l+1}, \mathbf{x}_{l+2}, \ldots, \mathbf{x}_{l+u}]$ as unlabeled data. In the original dataset $\mathbf{X}$, the input dataset $\mathbf{X} = [\mathbf{x}_1, \mathbf{x}_2, \cdots, \mathbf{x}_n] \in \mathbf{R}^{m\times n}$ is mapped to a high dimensional feature space $\mathbf{\Phi}(\mathbf{X}) = [\mathbf{\Phi}(\mathbf{x}_1), \mathbf{\Phi}(\mathbf{x}_2), \cdots, \mathbf{\Phi}(\mathbf{x}_n)]$, where n is the number of samples, $n = l + u$, m is the dimension of measurement variables.

(1) It is modified in the first step of KLLE algorithm. Firstly, in order to obtain more accurate reconstructed weight matrix, the weighted distance is employed to solve the neighborhood of the sample points.

Weighted distance as follows,

$$\mathbf{z}(\mathbf{\Phi}(\mathbf{x}_i), \mathbf{\Phi}(\mathbf{x}_j)) = \frac{\sqrt{\left\|\mathbf{\Phi}(\mathbf{x}_i)-\mathbf{\Phi}(\mathbf{x}_j)\right\|^2}}{\sqrt{\mathbf{S}(i)}\sqrt{\mathbf{S}(j)}} \tag{3}$$

Where $\mathbf{S}(i)$ denotes the mean of distance sum of the point $\mathbf{\Phi}(\mathbf{x}_i)$ to each point in their nearest neighbors. The $\mathbf{S}(j)$ denotes the mean of distance sum of the point $\mathbf{\Phi}(\mathbf{x}_j)$ to each point in their nearest neighbors.

Let

$$\mathbf{S}(i) = \frac{1}{k}\sum_{p=1}^{k}\left\|\mathbf{\Phi}\left(\mathbf{x}_i\right)-\mathbf{\Phi}\left(\mathbf{x}_p^i\right)\right\|^2,$$

$$\mathbf{S}(j) = \frac{1}{k}\sum_{q=1}^{k}\left\|\mathbf{\Phi}\left(\mathbf{x}_j\right)-\mathbf{\Phi}\left(\mathbf{x}_q^i\right)\right\|^2$$

Where $\mathbf{\Phi}\left(\mathbf{x}_p^i\right)$ $(p = 1, 2, \ldots, k)$ is the pth neighboring points of $\mathbf{\Phi}(\mathbf{x}_i)$, $\mathbf{\Phi}\left(\mathbf{x}_q^i\right)$ $(q = 1, 2, \ldots, k)$ is the qth neighboring points of $\mathbf{\Phi}\left(\mathbf{x}_j\right)$. The formula of $\sqrt{\mathbf{S}(i)}\sqrt{\mathbf{S}(j)}$ is shown at the top of this page. Where $\mathbf{K}\left(\mathbf{x}_i, \mathbf{x}_j\right) = \mathbf{\Phi}^T(\mathbf{x}_i)\,\mathbf{\Phi}\left(\mathbf{x}_j\right)$.

The new weighted distance can be defined as:

$$\mathbf{z}(\mathbf{\Phi}(\mathbf{x}_i), \mathbf{\Phi}(\mathbf{x}_j)) = \frac{\sqrt{\mathbf{K}_{ii}-2\mathbf{K}_{ij}+\mathbf{K}_{jj}}}{\sqrt{\Delta}} \tag{4}$$

For the sake of making full use of multiple classes data, the approach proposed in this paper combines the sample class information to compute the nearest neighbor of the sample points.

$$\mathbf{Z}_{ij} = \begin{cases}\mathbf{z}(\mathbf{\Phi}(\mathbf{x}_i), \mathbf{\Phi}(\mathbf{x}_j)) - r\mathbf{z}(\mathbf{\Phi}(\mathbf{x}_i), \mathbf{\Phi}(\mathbf{x}_j)) & \mathbf{x}_i, \mathbf{x}_j \text{ same class} \\ \mathbf{z}(\mathbf{\Phi}(\mathbf{x}_i), \mathbf{\Phi}(\mathbf{x}_j)) + r\mathbf{z}(\mathbf{\Phi}(\mathbf{x}_i), \mathbf{\Phi}(\mathbf{x}_j)) & \mathbf{x}_i, \mathbf{x}_j \text{ different class} \\ \mathbf{z}(\mathbf{\Phi}(\mathbf{x}_i), \mathbf{\Phi}(\mathbf{x}_j)) & \text{others}\end{cases} \tag{5}$$

Where, r is the adjustment factor, which is used to adjust the likelihood of labeled samples and unlabeled samples in the LLE method when they are chosen as nearest neighbors.

A new neighborhood is reconstructed by improved distance formula. Then the second and third steps of the algorithm is computed.

(2) Compute the reconstruction weights matrix $\mathbf{W}_{ij}$.

Because of introducing the regularization constraint $\lambda\|w\|^2$, the noise sensitivity is reduced. The new reconstruction error is obtained by cost function:

$$\begin{aligned}&\min\ e(\mathbf{W}) = \sum_{i=1}^{n}\left(\left\|\mathbf{\Phi}\left(\mathbf{x}_i\right)-\sum_{j=i}^{k}\mathbf{W}_{ij}\mathbf{\Phi}\left(\mathbf{x}_j\right)\right\|^2+\lambda\sum_{j=i}^{k}\mathbf{W}_{ij}^2\right) \\ &s.t.\begin{cases}\sum_{j=i}^{k}\mathbf{W}_{ij} = 1 \\ \mathbf{W}_{ij} = 0, \quad \mathbf{\Phi}\left(\mathbf{x}_j\right) \notin N_k\left(\mathbf{\Phi}\left(\mathbf{x}_i\right)\right),\ i = 1, 2, \ldots, n\end{cases}\end{aligned} \tag{6}$$

(3) The sample points are mapped to low dimensional space.

In the interest of acquire the local and global information of the data space, the global idea of KPCA is introduced into the objective function. Suppose that $\mathbf{F}$ is a projection matrix mapped to low dimensional space. The optimization objective function of the KPCA can be expressed by the maximal variance of the projection coordinates [26], [27]. Let low-dimensional coordinates $\mathbf{V}(\mathbf{X}) = \mathbf{F}^T\mathbf{\Phi}(\mathbf{X})$.

$$\max\ J_{KPCA} = \max\ \frac{1}{n}\mathbf{V}(\mathbf{X})\,\mathbf{V}(\mathbf{X})^T \tag{7}$$

The projection matrix is found through the new minimized objective function:

$$\begin{aligned}
&\min \ (\alpha e\left(\mathbf{V}\left(\mathbf{x}\right)\right)-\left(1-\alpha\right)J_{KPCA}) \\
&\quad=\alpha\sum_{i=1}^{n}\left\|\mathbf{V}\left(x_i\right)-\sum_{j=1}^{n}\mathbf{W}_{ij}\mathbf{V}\left(\mathbf{x}_j\right)\right\|^2 \\
&\qquad-\left(1-\alpha\right)\mathbf{F}^T\mathbf{C}_{\Phi}\mathbf{F} \\
&\quad=\alpha\sum_{i=1}^{n}\left\|\mathbf{F}^T\mathbf{\Phi}\left(\mathbf{x}_i\right)-\sum_{j=1}^{n}\mathbf{W}_{ij}\mathbf{F}^T\mathbf{\Phi}\left(\mathbf{x}_j\right)\right\|^2 \\
&\qquad-\left(1-\alpha\right)\mathbf{F}^T\left(\frac{1}{n}\sum_{i=1}^{n}\mathbf{\Phi}\left(\mathbf{x}_i\right)\mathbf{\Phi}^T\left(\mathbf{x}_i\right)\right)\mathbf{F} \\
&\quad=trace(\alpha\left(\mathbf{F}^T\mathbf{\Phi}\left(\mathbf{X}\right)\mathbf{M}\mathbf{\Phi}^T\left(\mathbf{X}\right)\mathbf{F}\right) \\
&\qquad-\frac{1-\alpha}{n}\mathbf{F}^T\mathbf{\Phi}\left(\mathbf{X}\right)\mathbf{\Phi}^T\left(\mathbf{X}\right)\mathbf{F}) \\
&s.t.\ \mathbf{F}^T\mathbf{F}=\mathbf{I}
\end{aligned}\tag{8}$$

Where $\mathbf{M}=\mathbf{M}^T=\left(\mathbf{I}-\mathbf{W}\right)^T\left(\mathbf{I}-\mathbf{W}\right)$.

It is derived by Lagrange multiplier method:

$$\begin{aligned}
L&=trace(\alpha\left(\mathbf{F}^T\mathbf{\Phi}\left(\mathbf{X}\right)\mathbf{M}\mathbf{\Phi}^T\left(\mathbf{X}\right)\mathbf{F}\right) \\
&\quad-\frac{1-\alpha}{n}\mathbf{F}^T\mathbf{\Phi}\left(\mathbf{X}\right)\mathbf{\Phi}^T\left(\mathbf{X}\right)\mathbf{F})-\lambda\left(\mathbf{F}^T\mathbf{F}-\mathbf{I}\right) \\
\frac{\partial L}{\partial\mathbf{F}}&=\alpha\mathbf{\Phi}\left(\mathbf{X}\right)\mathbf{M}\mathbf{\Phi}^T\left(\mathbf{X}\right)\mathbf{F}+\alpha\left(\mathbf{\Phi}\left(\mathbf{X}\right)\mathbf{M}\mathbf{\Phi}^T\left(\mathbf{X}\right)\right)^T\mathbf{F} \\
&\quad-\frac{1-\alpha}{n}\mathbf{\Phi}\left(\mathbf{X}\right)\mathbf{\Phi}^T\left(\mathbf{X}\right)\mathbf{F} \\
&\quad-\frac{1-\alpha}{n}\left(\mathbf{\Phi}\left(\mathbf{X}\right)\mathbf{\Phi}^T\left(\mathbf{X}\right)\right)^T\mathbf{F}-2\lambda\mathbf{F} \\
&=\mathbf{0} \\
\frac{\partial L}{\partial\lambda}&=\mathbf{F}^T\mathbf{F}-\mathbf{I}=0
\end{aligned}\tag{9}$$

Let $\mathbf{F}=\mathbf{\Phi}\left(\mathbf{X}\right)\mathbf{T}$, $\mathbf{T}=[\mathbf{t}_1,\mathbf{t}_2,\ldots,\mathbf{t}_m]\in\mathbf{R}^n$ is the coefficient matrix.

The above formula can be converted to,

$$\begin{aligned}
\alpha\mathbf{\Phi}\left(\mathbf{X}\right)\mathbf{M}\mathbf{\Phi}^T\left(\mathbf{X}\right)\mathbf{\Phi}\left(\mathbf{X}\right)\mathbf{T}-\frac{1-\alpha}{n}\mathbf{\Phi}\left(\mathbf{X}\right)\mathbf{\Phi}^T\left(\mathbf{X}\right)\mathbf{\Phi}\left(\mathbf{X}\right)\mathbf{T} \\
=\lambda\mathbf{\Phi}\left(\mathbf{X}\right)\mathbf{T}
\end{aligned}\tag{10}$$

The above formula is left multiplied $\mathbf{\Phi}'^T\left(\mathbf{X}\right)$ as follow:

$$\begin{aligned}
&\alpha\mathbf{\Phi}^T\left(\mathbf{X}\right)\mathbf{\Phi}\left(\mathbf{X}\right)\mathbf{M}\mathbf{\Phi}^T\left(\mathbf{X}\right)\mathbf{\Phi}\left(\mathbf{X}\right)\mathbf{T} \\
&\quad-\frac{1-\alpha}{n}\mathbf{\Phi}^T\left(\mathbf{X}\right)\mathbf{\Phi}\left(\mathbf{X}\right)\mathbf{\Phi}^T\left(\mathbf{X}\right)\mathbf{\Phi}\left(\mathbf{X}\right)\mathbf{T} \\
&=\lambda\mathbf{\Phi}^T\left(\mathbf{X}\right)\mathbf{\Phi}\left(\mathbf{X}\right)\mathbf{T}
\end{aligned}\tag{11}$$

The new generalized characteristic equation as follow:

$$\alpha\mathbf{KMKT}-\frac{1-\alpha}{n}\mathbf{KKT}=\lambda\mathbf{KT}\tag{12}$$

The matrix $\mathbf{T}$ is achieved by solving the generalized eigenvalue equation. Therefore the coordinates of low dimensional space is obtained by (11). This parameter α is determined by prior knowledge.

$$\begin{aligned}
\mathbf{V}(\mathbf{x})&=\mathbf{F}^T\mathbf{\Phi}\left(\mathbf{x}\right) \\
&=\mathbf{T}^T\mathbf{\Phi}^T\left(\mathbf{x}\right)\mathbf{\Phi}\left(\mathbf{x}\right) \\
&=\mathbf{T}^T\mathbf{K}\left(\mathbf{x},\mathbf{x}\right)
\end{aligned}\tag{13}$$

The T^2 and *SPE* statistics are defined and the corresponding control limits are as follows,

$$T^2=t^T\Lambda^{-1}t\le\frac{A(n^2-1)}{n(n-A)}F_{A,n-A;\alpha}\tag{14}$$

$$SPE=\|x\|^2\le g\chi^2_{h;\alpha}\tag{15}$$

Where, $F_{A,n-A;\alpha}$ is the F distribution with confidence levels of α, and the $g\chi^2_{h;\alpha}$ conforms to χ^2 distribution with scale factor g, degree of freedom h and confidence level α.

IV. PROCESS MONITORING METHOD BASED ON MK-SSLLE

The process monitoring method based on MK-SSLLE is divided into two stages: off-line modeling and on-line fault monitoring. In the off-line modeling stage, the MK-SSLLE method is used to establish the model of normal operating conditions. The monitoring statistics are T^2 statistics and *SPE* statistics.

Assume that the on-line standardized process data is $\mathbf{\Phi}\left(\mathbf{x}_o\right)$. Therefore, the coordinates of low dimensional space as follow:

$$\begin{aligned}
\mathbf{H}_o&=\mathbf{F}^T\mathbf{\Phi}\left(\mathbf{X}_o\right) \\
&=\mathbf{T}^T\mathbf{\Phi}^T\left(\mathbf{X}\right)\mathbf{\Phi}\left(\mathbf{X}_o\right) \\
&=\mathbf{T}^T\mathbf{K}\left(\mathbf{X},\mathbf{X}_o\right)
\end{aligned}\tag{16}$$

The T^2 statistics as follow:

$$\begin{aligned}
T_o^2&=\mathbf{H}_o^T\mathbf{\Lambda}^{-1}\mathbf{H}_o \\
&=\left(\mathbf{F}^T\mathbf{\Phi}\left(\mathbf{X}_o\right)\right)^T\mathbf{\Lambda}^{-1}\mathbf{F}^T\mathbf{\Phi}\left(\mathbf{X}_o\right) \\
&=\mathbf{\Phi}^T\left(\mathbf{X}_o\right)\mathbf{\Phi}\left(\mathbf{X}\right)\mathbf{T}\mathbf{\Lambda}^{-1}\mathbf{T}^T\mathbf{\Phi}^T\left(\mathbf{X}\right)\mathbf{\Phi}\left(\mathbf{X}_o\right) \\
&=\mathbf{K}\left(\mathbf{X}_o,\mathbf{X}\right)\mathbf{T}\mathbf{\Lambda}^{-1}\mathbf{T}^T\mathbf{K}\left(\mathbf{X},\mathbf{X}_o\right) \\
&=\mathbf{K}_{\mathbf{X}_o,\mathbf{X}}\mathbf{T}\mathbf{\Lambda}^{-1}\mathbf{T}^T\mathbf{K}_{\mathbf{X},\mathbf{X}_o}
\end{aligned}\tag{17}$$

Where

$$\begin{aligned}
\Lambda&=\frac{1}{n-1}\mathbf{V}^T\left(\mathbf{x}\right)\mathbf{V}\left(\mathbf{x}\right) \\
&=\frac{1}{n-1}\mathbf{\Phi}^T\left(\mathbf{x}\right)\mathbf{F}\mathbf{F}^T\mathbf{\Phi}\left(\mathbf{x}\right).
\end{aligned}$$

The *SPE* statistics as follow:

$$\begin{aligned}
SPE_o&=\left\|\tilde{\mathbf{\Phi}}\left(\mathbf{X}_{new}\right)\right\|^2=\left\|\left(\mathbf{\Phi}^T\left(\mathbf{X}_o\right)-\mathbf{H}_o^T\mathbf{F}^T\right)\right\|^2 \\
&=\left\|\mathbf{\Phi}^T\left(\mathbf{X}_o\right)\left(\mathbf{I}-\mathbf{\Phi}\left(\mathbf{X}\right)\mathbf{T}\mathbf{T}^T\mathbf{\Phi}^T\left(\mathbf{X}\right)\right)\right\|^2 \\
&=\left\|\left(\mathbf{I}-\mathbf{\Phi}\left(\mathbf{X}\right)\mathbf{T}\mathbf{T}^T\mathbf{\Phi}^T\left(\mathbf{X}\right)\right)\mathbf{\Phi}\left(\mathbf{X}_o\right)\right\|^2 \\
&=\mathbf{\Phi}^T(\mathbf{X}_o)(\mathbf{I}-2\mathbf{\Phi}(\mathbf{X})\mathbf{T}\mathbf{T}^T\mathbf{\Phi}^T(\mathbf{X}) \\
&\quad+\mathbf{\Phi}(\mathbf{X})\mathbf{T}\mathbf{T}^T\mathbf{\Phi}^T(\mathbf{X})\mathbf{\Phi}(\mathbf{X})\mathbf{T}\mathbf{T}^T\mathbf{\Phi}^T(\mathbf{X}))\mathbf{\Phi}(\mathbf{X}_o)
\end{aligned}$$

$$= \mathbf{K}(\mathbf{X}_o, \mathbf{X}_o) - 2\mathbf{K}(\mathbf{X}_o, \mathbf{X})\mathbf{T}\mathbf{T}^T\mathbf{K}(\mathbf{X}, \mathbf{X}_o) + \mathbf{K}(\mathbf{X}_o, \mathbf{X})\mathbf{T}\mathbf{T}^T\mathbf{K}(\mathbf{X}, \mathbf{X})\mathbf{T}\mathbf{T}^T\mathbf{K}(\mathbf{X}, \mathbf{X}_o) = \mathbf{K}_{\mathbf{X}_o,\mathbf{X}_o} - 2\mathbf{K}_{\mathbf{X}_o,\mathbf{X}}\mathbf{T}\mathbf{T}^T\mathbf{K}_{\mathbf{X},\mathbf{X}}\mathbf{T}\mathbf{T}^T\mathbf{K}_{\mathbf{X},\mathbf{X}_o} \quad (18)$$

The specific steps of offline modeling as follows:

(1) Standardized processing for the data sets $\mathbf{X}$.

(2) By introducing the kernel function, the data sets $\mathbf{X}$ is mapped to a high dimensional space $F : \mathbf{X} \rightarrow \mathbf{\Phi}(\mathbf{X})$.

(3) Calculate projection matrix $\mathbf{F}$ and coefficient matrix $\mathbf{T}$ by MK-SSLLE algorithm.

(4) Determine the control limits of T^2 statistic and *SPE* statistic.

The specific steps of online monitoring are as follows:

(1) Standardized processing for the new data sets x_o.

(2) Compute new kernel function $\mathbf{K}_{new}, \mathbf{K}_{new} = \mathbf{K}(\mathbf{x}_o, \mathbf{x}_j)$, where $x_j\ j = 1, 2, \ldots, n$.

(3) Compute the coordinates of low dimensional space $\mathbf{H}_o$.

(4) Calculate T^2 statistic and *SPE* statistic.

(5) If T^2 statistic and *SPE* statistic exceed their respective control limits, the fault may occur, otherwise the new sample is normal.

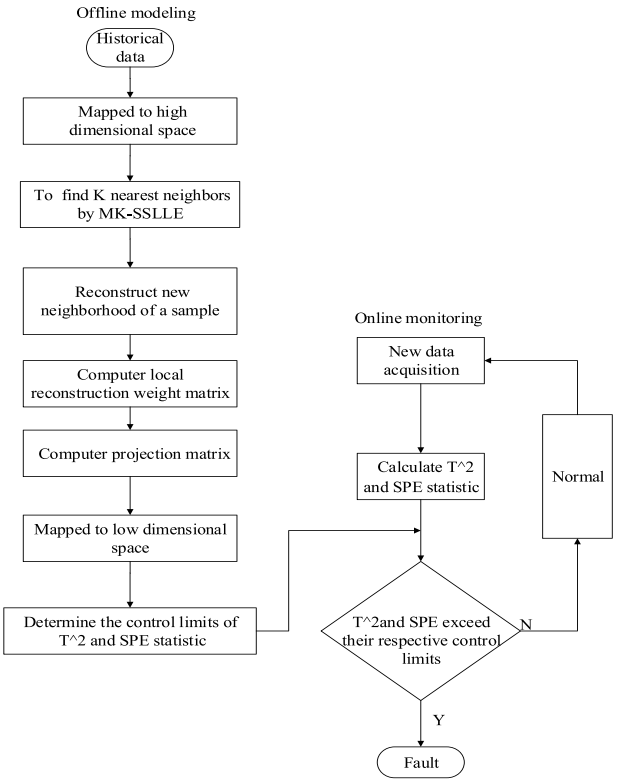

FIGURE 2. The flow chart of process monitoring based on MK-SSLLE method.

Process monitoring flow chart for MK-SSLLE algorithm as follow Fig. 2.

V. EXPERIMENTAL RESEARCH AND RESULT ANALYSIS

A. PRODUCTION PROCESS OF FUSED MAGNESIA

Electrical fused magnesia furnace (EFMF) is one of the main equipment for the production of fused magnesia. The main component of fused magnesia for magnesia, and the magnesia is a kind of important refractory material. It has already gotten extensive application in chemical industry, metallurgy, aerospace and many other industrial fields in recent years. Now the magnesia is produced mainly by the electrical smelting magnesium furnace equipment, and the raw materials is mainly magnesite or light burned magnesium. The bulk magnesite is selected as raw material in this paper.

It takes full advantage of the arc between the charge and electrode to produce energy to melt the raw material. The fused magnesium crystal with higher purity is obtained. The composition of each part of the electrical smelting magnesium furnace equipment are shown in Fig. 3. The main equipment of electric melting magnesium furnace is transformer, electrode, lifting device, furnace shell and so on.

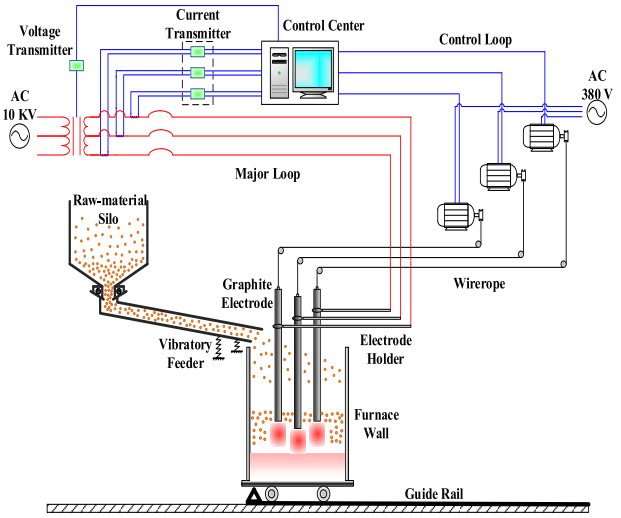

FIGURE 3. Diagram of electrical fused magnesium furnace.

The degree of automation of the electrical smelting magnesium furnace is usually low in our country, and it is very easy to produce fault and abnormal phenomenon. Therefore, it is very necessary and significant to detect the abnormality and fault in the working process.

B. SIMULATION RESULTS ANALYSIS

In order to solve the abnormal working conditions and faults in the smelting process, the MK-SSLLE method is applied to the fault detection in the production process.

Fault types are mainly fault 1 and fault 2. Fault 1 is defined as follows. In the process of production, the gas pressure in the furnace will be out of balance due to the emission of the gas, when the current setting value is constant and the particle size of the raw material is relatively large changes. This phenomenon will cause the drastic fluctuations of electrodes and molten pool liquid level, so that the melt is erupted out of the furnace with gas. The furnace eruption working condition is used as a fault 1 in this paper. Fault 2 is defined as follows. As the furnace wall is overheated, the furnace wall melts. After that the melt flows out of the furnace. This leak furnace working conditions is used as a fault 2 in this paper.

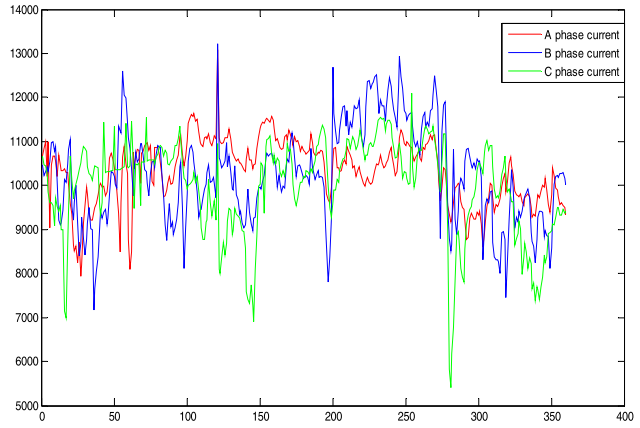

FIGURE 4. current Sample points for testing MK-SSLLE.

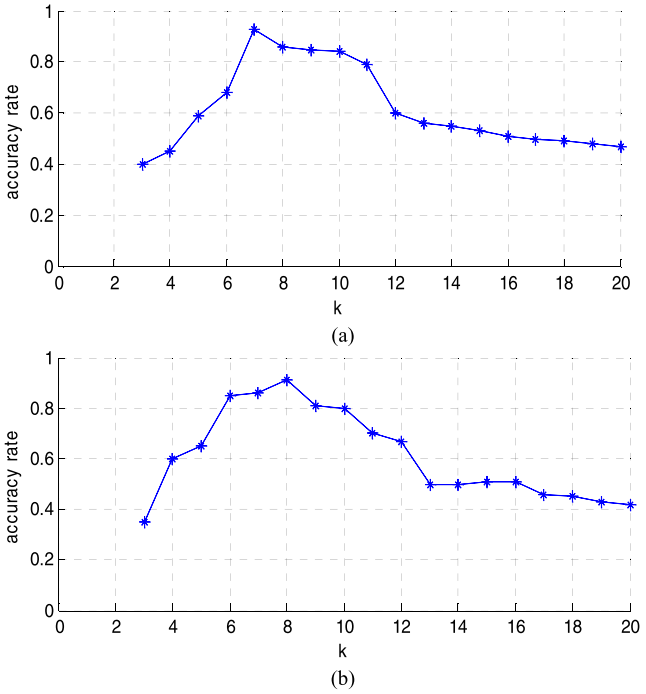

FIGURE 5. Performance with different k value based on MK-SSLLE. (a) Fault 1. (b) Fault 2.

Multi-mode normal data are produced in the production of Magnesium Oxide. For example, some mode categories, manual feeding and automatic feeding switching, different feed rates. There are six variables: A phase voltage and current, B phase voltage and current and C phase voltage and current. The training set and the test set select 360 samples, respectively. Where, the training set contains 200 labeled data and 160 unlabeled data. Three phase current as shown in Fig. 4. The abscissa represents the moment, and the ordinate represents the current.

In the process monitoring based on MK-SSLLE method, k is an important parameter of the algorithm, which directly affects the solution of the objective function in the MK-SSLLE method. So far, there is no uniform method for the selection of the nearest neighbor parameters. In this part, two kinds of faults are taken as examples, and the relationship between the k value of different parameters and the performance of process monitoring is described.

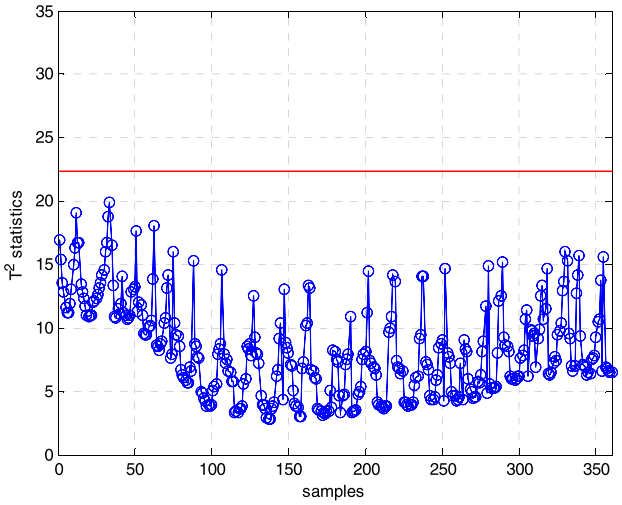

FIGURE 6. Offline KLLE T^2 statistics.

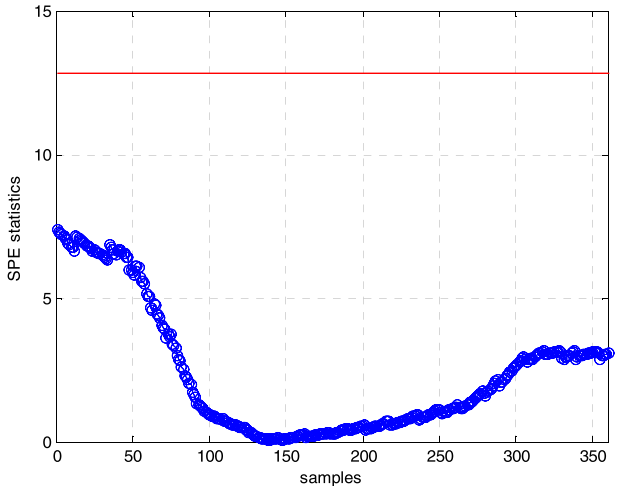

FIGURE 7. Offline KLLE *SPE* statistics.

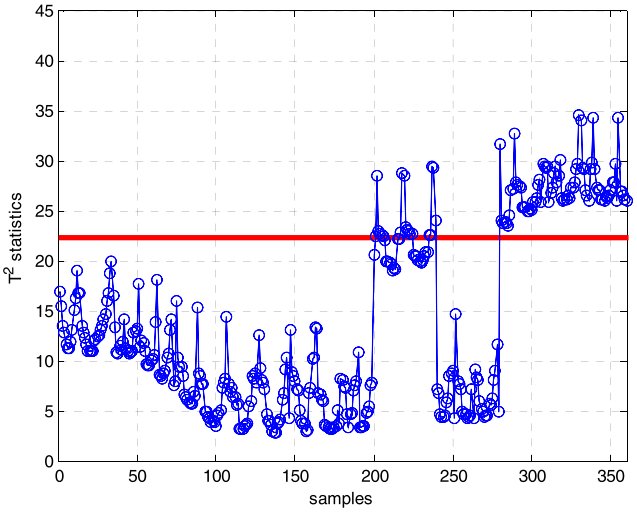

FIGURE 8. On-line KLLE T^2 statistics of fault 1.

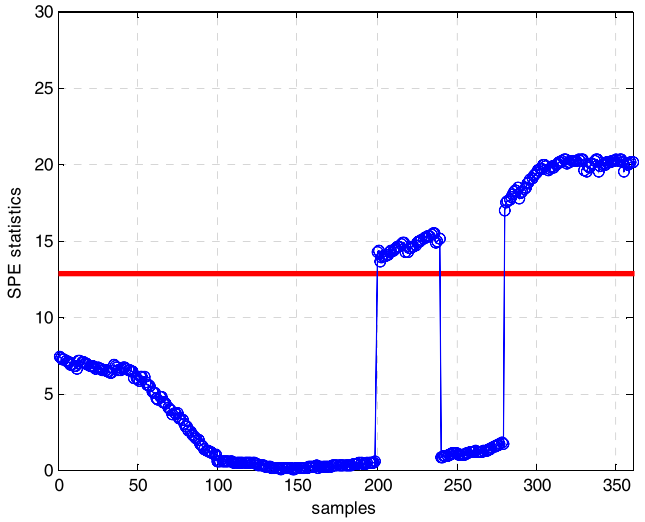

FIGURE 9. On-line KLLE *SPE* statistics of fault 1.

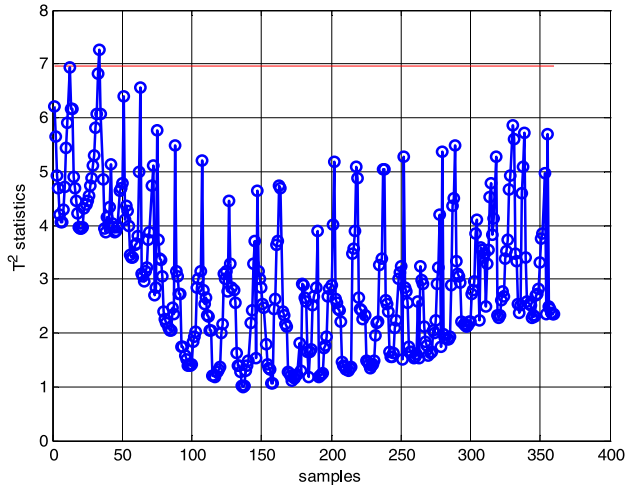

FIGURE 10. Offline MK-SSLLE T^2 statistics.

The Fig.5 shows that the optimal value of k is different for different faults. However, as an actual process monitoring, it is impossible to predict the fault type, so the parameter k is approximate value.

In order to demonstrate the detection performance of MK-SSLLE and compare other methods, in this section T^2 and *SPE* statistics are used as the detection indicators. The T^2 and *SPE* of the two methods are listed in Fig. 6-15.

As can be seen from Fig. 6-9, the fault can be detected in time by *SPE* statistics, and the T^2 statistics could not be accurate and reliable to detect the fault of two time periods.

The KLLE algorithm can't preserve the global structure of the data while considering the manifold structure between the local nearest neighbor points.

As can be known from Fig.10-13, the fault 1 can be completely detected by the MK-SSLLE. Moreover, the proposed method has superior detection performance over two time periods.

According to the monitoring chart Fig.14 and Fig.15, the fault 2 can also be detected in a timely by means of *SPE* statistics and T^2 statistics.

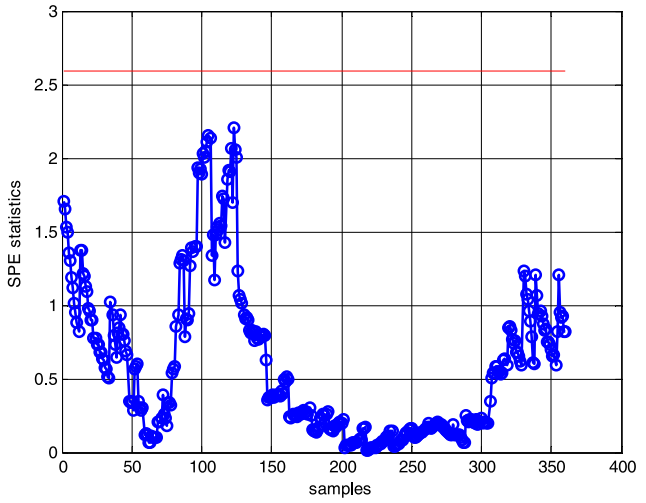

FIGURE 11. Offline MK-SSLLE *SPE* statistics.

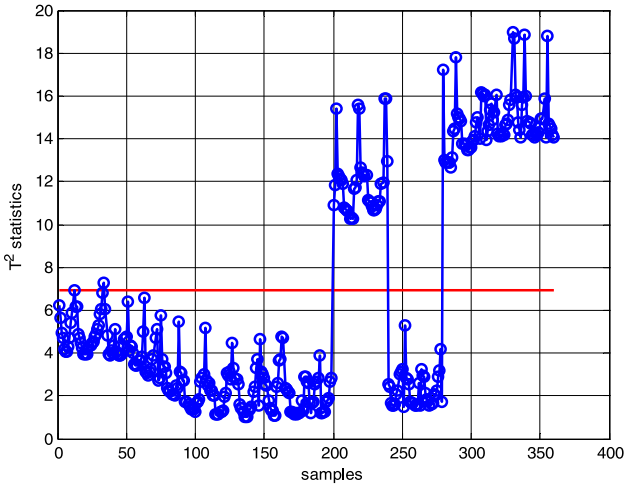

FIGURE 12. On-line MK-SSLLE T^2 statistics of fault 1.

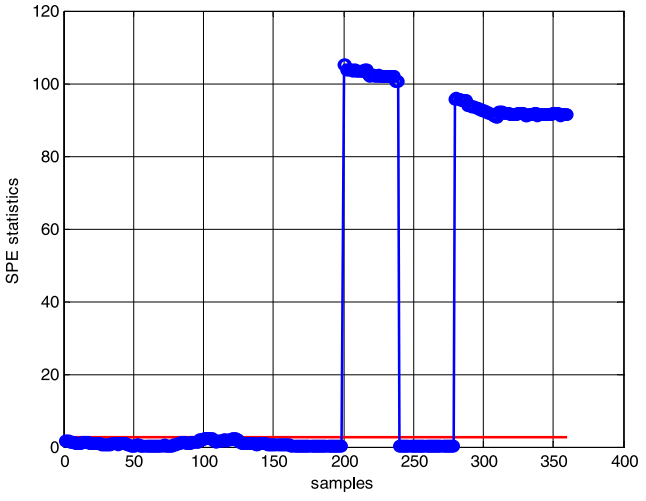

FIGURE 13. On-line MK-SSLLE *SPE* statistic of fault 1.

Obviously, it can be demonstrated that the KLLE method is false positives, and the proposed MK-SSLLE method can detect faults accurately and timely. The global

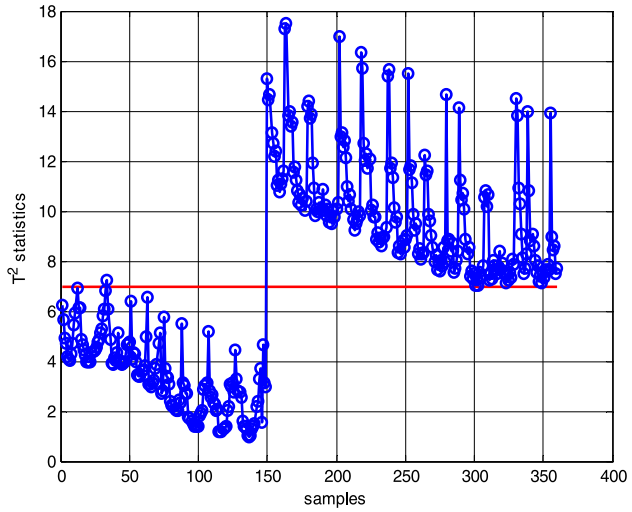

FIGURE 14. On-line MK-SSLLE T^2 statistics of fault 2.

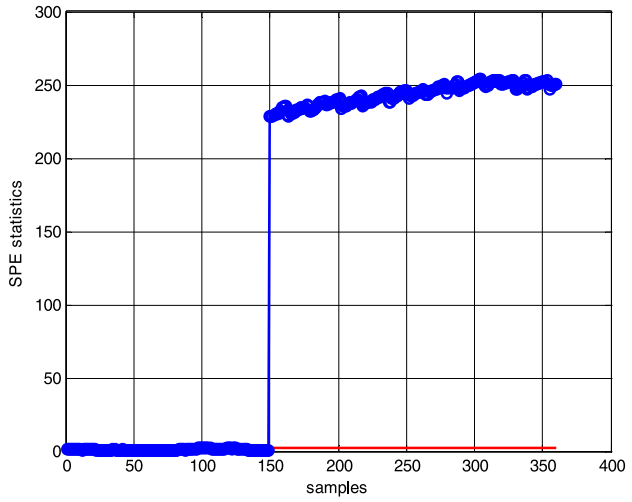

FIGURE 15. On-line MK-SSLLE *SPE* statistic of fault 2.

TABLE 1. Indicators of different methods.

fault	method	statistic	accuracy rate	false alarm rate	Missing alarm rate
1	KLLE	T^2	94.13	4.74	2.23
		SPE	93.35	3.83	4.93
	MK-SSLLE	T^2	99.62	0.06	0.11
		SPE	99.71	0.25	0.01
2	KLLE	T^2	93.91	3.06	5.05
		SPE	93.42	2.99	4.71
	MK-SSLLE	T^2	99.79	0.03	0.16
		SPE	99.81	0.32	0.06

structure information and the local structure information of the data are important information of the original sampling data. As mentioned above, the MK-SSLLE algorithm can extract the local manifold structure and global feature information in the process of data dimension reduction. Furthermore, it can make full use of the prior information of a small amount of labeled samples in the training samples, and capture the most important information in the dataset. Therefore, the MK-SSLLE algorithm exhibits an efficient detection performance.

The accuracy rate, false alarm rate and missing alarm rate of KLLE and MK-SSLLE for fused magnesia furnace process monitoring as depicted in Table 1. The experimental results indicate that the proposed method is feasible and the method has an ascendant monitoring effect in the real-time monitoring of the industrial production status of the fused magnesia furnace.

VI. CONCLUSIONS

In this paper, a new EFMF monitoring approach based on modified kernel semi-supervised local linear embedding is presented. To begin with, the proposed method utilized partial label information to adjust the distance matrix to obtain nearest neighbors. Secondly, the method can fully extract the global structure information and the local manifold information for sample data. Finally, the proposed method has been verified that the satisfactory results of the detection by the experiment of electrical fused magnesia furnace.

REFERENCES

[1] S. Yin, X. Li, H. Gao, and O. Kaynak, "Data-based techniques focused on modern industry: An overview," *IEEE Trans. Ind. Electron.*, vol. 62, no. 1, pp. 657–667, Jan. 2015.

[2] J. J. Hong, J. Zhang, and J. Morris, "Fault localization in batch processes through progressive principal component analysis modeling," *Ind. Eng. Chem. Res.*, vol. 50, no. 13, pp. 8153–8162, 2011.

[3] Z. Ge and Z. Song, "Performance-driven ensemble learning ICA model for improved non-Gaussian process monitoring," *Chemometrics Intell. Lab. Syst.*, vol. 123, no. 2, pp. 1–8, 2013.

[4] G. Wang and S. Yin, "Quality-related fault detection approach based on orthogonal signal correction and modified PLS," *IEEE Trans. Ind. Informat.*, vol. 11, no. 2, pp. 398–405, Apr. 2015.

[5] Y. Zhang, H. Zhou, S. J. Qin, and T. Chai, "Decentralized fault diagnosis of large-scale processes using multiblock kernel partial least squares," *IEEE Trans. Ind. Informat.*, vol. 6, no. 1, pp. 3–10, Feb. 2010.

[6] Z. Ge, S. Zhong, and Y. Zhang, "Semisupervised kernel learning for FDA model and its application for fault classification in industrial processes," *IEEE Trans. Ind. Informat.*, vol. 12, no. 4, pp. 1403–1411, Aug. 2016.

[7] S. T. Roweis and L. K. Saul, "Nonlinear dimensionality reduction by locally linear embedding," *Science*, vol. 290, no. 5500, pp. 2323–2326, 2000.

[8] X. He, S. Yan, Y. Hu, P. Niyogi, and H.-J. Zhang, "Face recognition using laplacianfaces," *IEEE Trans. Pattern Anal. Mach. Intell.*, vol. 27, no. 3, pp. 328–340, Mar. 2005.

[9] D. L. Donoho and C. Grimes, "Hessian eigenmaps: Locally linear embedding techniques for high-dimensional data," *Proc. Nat. Acad. Sci. USA*, vol. 100, no. 10, pp. 5591–5596, 2003.

[10] C. F. Alcala and S. J. Qin, "Analysis and generalization of fault diagnosis methods for process monitoring," *J. Process. Control*, vol. 21, no. 3, pp. 322–330, 2011.

[11] B.-Y. Sun, X.-M. Zhang, X.-M. Mao, and J. Li, "Feature fusion using locally linear embedding for classification," *IEEE Trans. Neural Netw.*, vol. 21, no. 1, pp. 163–168, Jan. 2010.

[12] M. Wang, J. Yang, K.-C. Chou, and Z.-J. Xu, "SLLE for predicting membrane protein types," *J. Theor. Biol.*, vol. 232, no. 1, pp. 7–15, 2005.

[13] T. Tsagaroulis and A. B. Hamza, "Kernel locally linear embedding algorithm for quality control," in *Novel Algorithms and Techniques in Telecommunications, Automation and Industrial Electronics*. New York, NY, USA: Springer, 2008, pp. 1–6.
[14] R. Karbauskaitė, O. Kurasova, and G. Dzemyda, "Selection of the number of neighbours of each data point for the locally linear embedding algorithm," *Inf. Technol. Control*, vol. 36, no. 4, pp. 359–364, 2015.
[15] C.-Y. Cheng, C.-C. Hu, and M.-C. Chen, "Adaptive kernel principal component analysis (KPCA) for monitoring small disturbances of nonlinear processes," *Ind. Eng. Chem. Res.*, vol. 49, no. 5, pp. 2254–2262, 2011.
[16] L. Xie, Z. Li, U. Kruger, and J. Zeng, "Block adaptive kernel principal component analysis for nonlinear process monitoring," *AICHE J.*, vol. 62, no. 12, pp. 4334–4345, 2016.
[17] J. Zhang, J. Yu, J. You, D. Tao, N. Li, and J. Cheng, "Data-driven facial animation via semi-supervised local patch alignment," *Pattern Recognit.*, vol. 57, pp. 1–20, Sep. 2016.
[18] D. Liang, J. Yang, Z. Zheng, and Y. Chang, "A facial expression recognition system based on supervised locally linear embedding," *Pattern Recognit. Lett.*, vol. 26, no. 15, pp. 2374–2389, 2005.
[19] S. Yin, S. X. Ding, X. Xie, and H. Luo, "A review on basic data-driven approaches for industrial process monitoring," *IEEE Trans. Ind. Electron.*, vol. 61, no. 11, pp. 6418–6428, Nov. 2014.
[20] Y. Zhang, T. Chai, C. Yang, and Z. Li, "Modeling and monitoring of dynamic processes," *IEEE Trans. Neural Netw. Learn. Syst.*, vol. 23, no. 2, pp. 277–284, Feb. 2012.
[21] S. Yin, X. Zhu, and O. Kaynak, "Improved PLS focused on key-performance-indicator-related fault diagnosis," *IEEE Trans. Ind. Electron.*, vol. 62, no. 3, pp. 1651–1658, Mar. 2015.
[22] Y. W. Zhang and S. Li, "Modeling and monitoring between-mode transition of multimodes processes," *IEEE Trans. Ind. Informat.*, vol. 9, no. 4, pp. 2248–2255, Nov. 2013.
[23] A. Yeredor, "Independent component analysis over Galois fields of prime order," *IEEE Trans. Inf. Theory*, vol. 57, no. 8, pp. 5342–5359, Aug. 2011.
[24] Q. Liu, S. J. Qin, and T. Chai, "Decentralized fault diagnosis of continuous annealing processes based on multilevel PCA," *IEEE Trans. Autom. Sci. Eng.*, vol. 10, no. 3, pp. 687–698, Jul. 2013.
[25] H. Zhang, X. Tian, and X. Deng, "Batch process monitoring based on multiway global preserving kernel slow feature analysis," *IEEE Access*, vol. 5, pp. 2696–2710, 2017.
[26] J. M. Lee, C. Yoo, S. W. Choi, P. A. Vanrolleghem, and I.-B. Lee, "Nonlinear process monitoring using kernel principal component analysis," *Chem. Eng. Sci.*, vol. 59, no. 1, pp. 223–234, 2004.
[27] X. Deng, X. Tian, S. Chen, and C. J. Harris, "Fault discriminant enhanced kernel principal component analysis incorporating prior fault information for monitoring nonlinear processes," *Chemometrics Intell. Lab. Syst.*, vol. 162, pp. 21–34, Mar. 2017.

YINGWEI ZHANG (SM'12) received the double B.S. degree in automation and mathematics from the Harbin Institute of Technology, Harbin, China, in 1993, and the master's and Ph.D. degrees in control theory and control engineering from Northeastern University, Shenyang, China, in 1998 and 2000, respectively.

She was a Post-Doctoral Researcher with Northeastern University from 2001 to 2003, and was promoted to an Associate Professor in 2002. Since 2010, she has been a Professor with the State Laboratory of Synthesis Automation of Process Industry, Northeastern University. Her current research interests include modeling, fault detection, and diagnosis.

Dr. Zhang received the National Science Fund for Distinguished Young Scholars in 2013. She has received Changjiang Scholar by China's Ministry of Education in 2014.

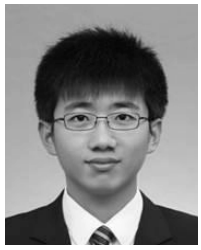

YUANJIAN FU received the B.S. degree in electrical engineering and automation from the Harbin University of Science and Technology, Weihai, China, in 2013, and the master's degree in control engineering from the Harbin University of Science and Technology, Harbin, China, in 2016. He is currently pursuing the Ph.D. degree in control theory and control engineering from Northeastern University, Shenyang, China.

His research interests include fault detection and fault diagnosis for complex industry processes.

ZHENBANG WANG received the B.S. degree in automation from Northeastern University in 2016. He is currently pursuing the master's degree in control theory and control engineering from Northeastern University, Shenyang, China.

His research interests include data modeling and fault diagnosis for large-scale industrial process.

LIN FENG received the B.S. degree in automation from Northeastern University in 2001, and the master's and Ph.D. degrees in control theory and control engineering from Northeastern University, Shenyang, China, in 2004 and 2013, respectively.

Her research interests include process monitoring and fault diagnosis for process industry.